Tetrahedron 70 (2014) 2784–2795

Contents lists available at ScienceDirect

Tetrahedron

journal homepage: www.elsevier.com/locate/tet

An experimental and theoretical study of the structure of Lamotrigine in its neutral and protonated forms: evidence of Lamotrigine enantiomers☆

Ibon Alkorta [a,*], José Elguero [a], Anna Font [b], Judit Galcera [c], Ignasi Mata [c], Elies Molins [c], Albert Virgili [b]

[a] Instituto de Química Médica (IQM-CSIC), Juan de la Cierva, 3, E-28006 Madrid, Spain
[b] Departament de Quìmica, Universitat Autònoma de Barcelona, Bellaterra, 08193 Cerdanyola, Barcelona, Spain
[c] Institut de Ciència de Materials de Barcelona (ICMAB-CSIC), Campus UAB, 08193 Bellaterra, Spain

ARTICLE INFO

Article history:
Received 10 January 2014
Received in revised form 18 February 2014
Accepted 26 February 2014
Available online 6 March 2014

Keywords:
Lamotrigine
X-ray crystallography
Dynamic NMR
Tautomerism
Axial chirality
GIAO calculations

ABSTRACT

The energies, geometries, and NMR chemical shifts have been calculated at the B3LYP/6-311++G(d,p) level for 17 structures of the anticonvulsant drug Lamotrigine and 29 structures of protonated Lamotrigine, including tautomers and *E*/*Z* isomers of the imino groups. The calculations were compared with solid state (X-ray and CPMAS NMR) and solution experimental results both reported in the literature and determined in this work. The conclusion is that Lamotrigine exists as the diamino tautomer and that its protonation takes place on the N2 atom. Using ABTE and/or deuterated ABTE as chiral solvating agent, it has been demonstrated for the first time by NMR in solution that Lamotrigine is a racemate of rapidly interconverting enantiomers. The crystal structure of two new solvated salts of Lamotrigine, both saccharinates, has been determined. Both salts present the same arrangement in chains of Lamotrigine and saccharinate joined by hydrogen bonds and stacking interactions. No isostructurality is present because of the different arrangement of the chains in both crystal structures.

1. Introduction

There is no need for a long introduction justifying the importance of Lamotrigine **1** (Lamictal, GlaxoSmithKline) since it is the treatment of choice for two serious illnesses: epilepsy[1–4] and bipolar disorder.[5–8] It is what it is known by the name of 'stand alone' drug. There is a 2012 review on Lamotrigine that covers all its known properties at that time.[9]

From that review,[9] and from a search in the literature, it appears that concerning Lamotrigine structural aspects, there is much information about X-ray crystallography (including polymorphism), some NMR data used to characterize it but almost none concerning computational studies. We have found only two papers. In the first one a molecular modeling study of Lamotrigine/β-cyclodextrin inclusion complex was carried out using the hybrid ONIOM2 method (the neutral diamino tautomer was used for the calculations).[10] In the second one, the IR and Raman spectra were calculated at the B3LYP/6-31G(d,p) level for the same tautomer.[11]

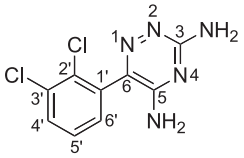

Lamotrigine **1** [6-(2,3-dichlorophenyl)-1,2,4-triazine-3,5-diamine]. We have numbered the dichlorophenyl group carbons 1' to 6' to distinguish the atoms of both rings.

☆ Dedicated to Professor Christian Roussel for his contributions to chirality

* Corresponding author. Tel.: +34 91 562 29 00; fax: +34 91 564 48 53; e-mail address: ibon@iqm.csic.es (I. Alkorta).
URL: http://www.iqm.csic.es/are

0040-4020/$ – see front matter © 2014 Elsevier Ltd. All rights reserved.
http://dx.doi.org/10.1016/j.tet.2014.02.075

The purpose of the present paper is to study theoretically the structure (tautomerism and isomerism) of Lamotrigine and its cation (relative energies) and calculate the chemical shifts of all structures. To support the calculations some new structures of Lamotrigine salts will be reported as well as the experimental determination of the barrier to enantiomerization.[12] In some papers, the name lamotriginium is used for protonated Lamotrigine. As with all international nonproprietary names (INNs) the WHO recommends to use always the INN without any modification: 'Names for different salts or esters of the same active substance should differ only with regard to the inactive moiety of the molecule'.[13]

We also want to determine if Lamotrigine axial chirality could be calculated and if enantiomerization barrier is high enough to be measured. The fact that Lamotrigine is a racemate has never been reported. Lamotrigine complexes with *S*,*S*-ABTE [(*S*,*S*)-α,α′–bis(trifluoromethyl)-9,10-anthracenedimethanol] could be of different energy and consequently the populations of both diastereoisomeric complexes could be not exactly 50/50. Considering that this difference should be very low and the interconversion between both complexes through free compounds very fast, we expected an equal distribution of enantiomers.

2. Results and discussion

2.1. Computational chemistry

2.1.1. Energies

2.1.1.1. Neutral Lamotrigine. Little is known about the tautomerism of amino-1,2,4-triazines; although the amino tautomers appear to be largely predominant, the participation of imino tautomers has been proposed.[14,15] Note that the presence of two tautomeric groups could favor the *exo* double-bonded tautomers, for instance whilst 3(5)-pyrazolinones are mixtures of oxo and hydroxy tautomers, 3,5-pyrazolidindiones are always dioxo ones.[14] Therefore, amino/imino tautomers were expected, a priori, to be relatively stable for Lamotrigine.

All possible isomers (excluding structural ones), both realistic and highly improbable, are represented in Fig. 1 and the corresponding dipole moments and relative energies are reported in Table 1.

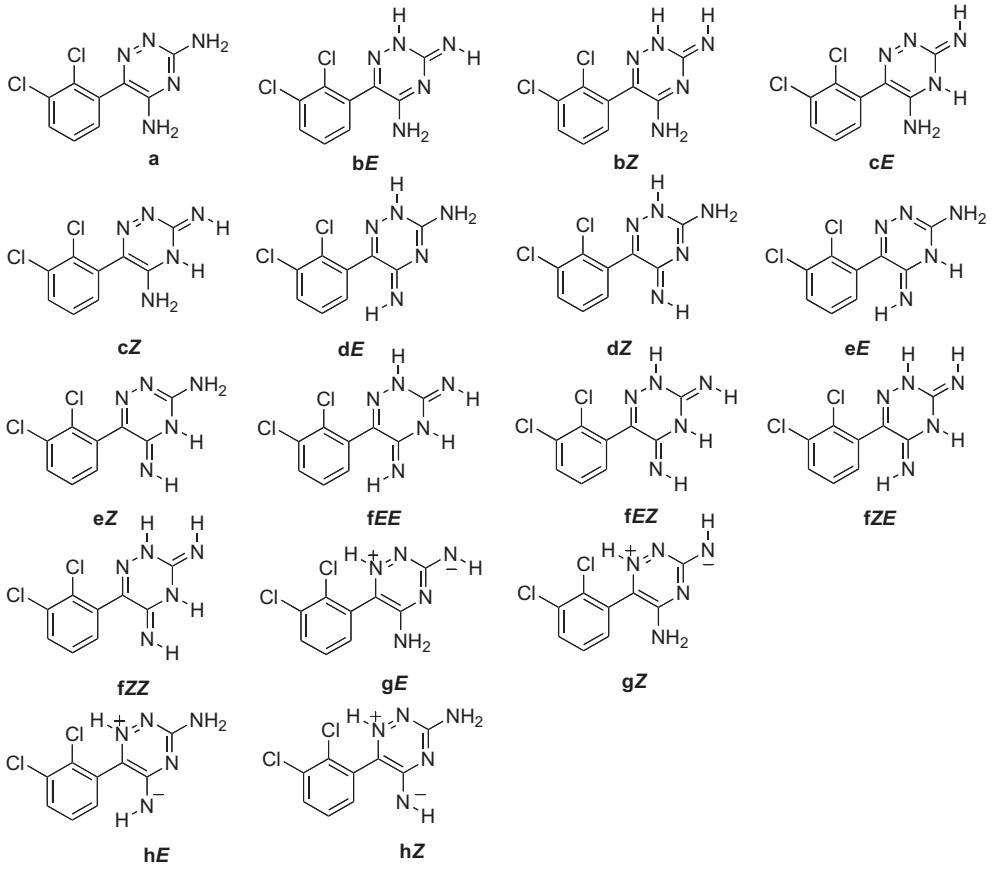

Fig. 1. The 17 isomers of Lamotrigine **1**.

The differences in energy are very important to the point that only tautomer **1a** (diamino) should exist; the next in energy is the **1b*E*** (3-imino/5-amino) that lies 38.0 kJ mol^{-1} higher. Note the large influence of the *E*/*Z* isomerism on the energies.

Table 1
Dipole moments (μ, Debye) and relative energies (kJ mol^{-1}) of the compounds of Fig. 1

Comp.	Dipole	E_{rel}	Comp.	Dipole	E_{rel}	Comp.	Dipole	E_{rel}
1a	3.16	0.0	**1d*Z***	6.13	55.8	**1f*ZZ***	3.16	74.3
1b*E*	5.03	38.0	**1e*E***	4.09	68.4	**1g*E***	7.99	136.7
1b*Z*	5.32	62.9	**1e*Z***	5.97	85.5	**1g*Z***	8.51	139.8
1c*E*	7.51	135.8	**1f*EE***	2.53	63.6	**1h*E***	4.84	110.8
1c*Z*	5.69	102.6	**1f*EZ***	2.83	76.3	**1h*Z***	4.18	90.4
1d*E*	5.68	70.3	**1f*ZE***	4.34	66.2			

2.1.1.2. Protonated Lamotrigine. All possible structures, tautomers as well as *E*/*Z* isomers, are represented in Fig. 2 whereas the corresponding relative energies are reported in Table 2.

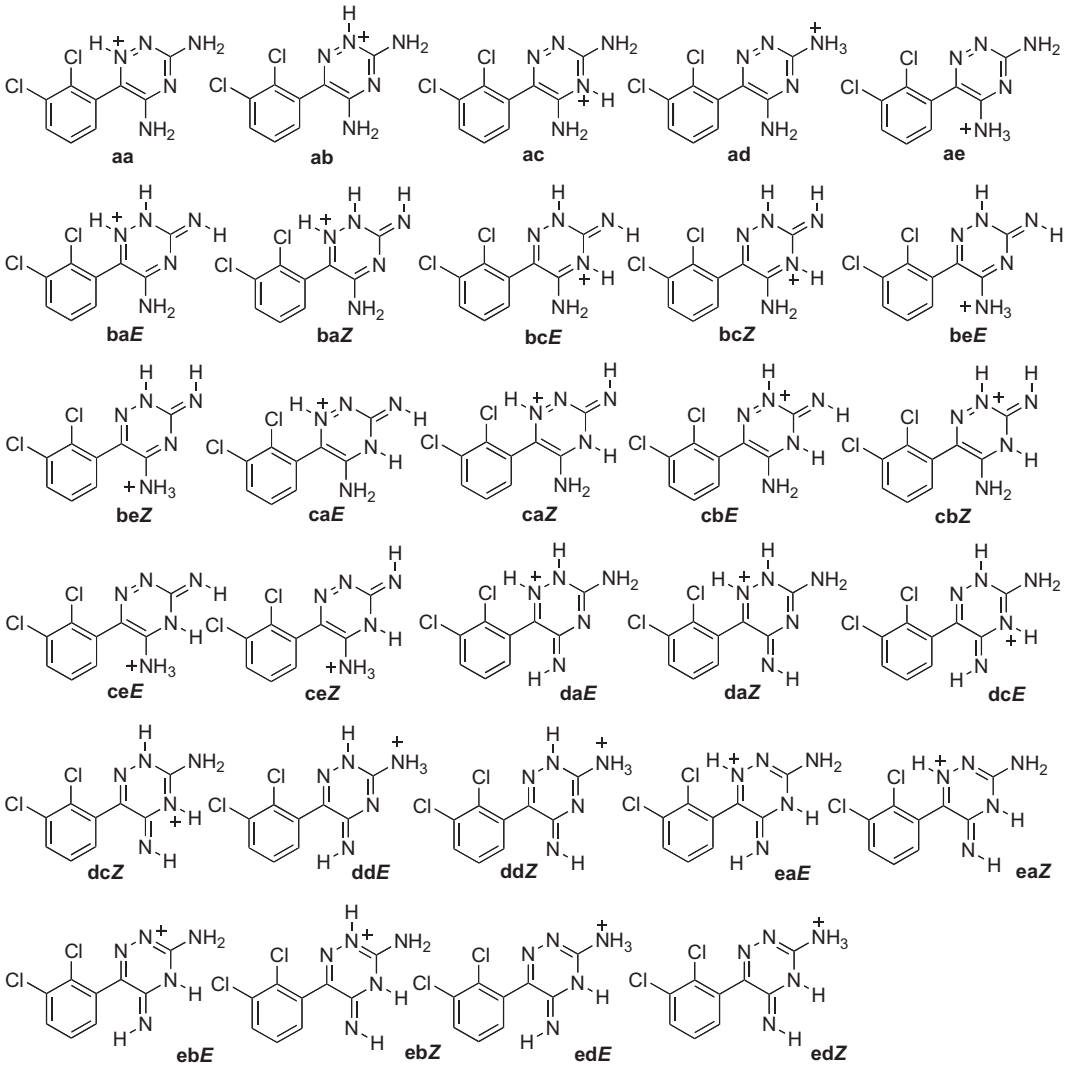

Fig. 2. The 29 isomers of protonated Lamotrigine.

Table 2
Relative energies (kJ mol^{-1}) of the isomers of Fig. 2

Comp.	E_{rel}	Comp.	E_{rel}	Comp.	E_{rel}
1H$^+$aa	21.2	**1H$^+$beZ**	208.7	**1H$^+$dcZ**	115.4
1H$^+$ab	0.0	**1H$^+$caE**	169.2	**1H$^+$ddE**	252.0
1H$^+$ac	88.7	**1H$^+$caZ**	141.0	**1H$^+$ddZ**	249.8
1H$^+$ad	120.3	**1H$^+$cbE**	99.5	**1H$^+$eaE**	97.1
1H$^+$ae	136.7	**1H$^+$cbZ**	90.6	**1H$^+$eaZ**	107.1
1H$^+$baE	174.6	**1H$^+$ceE**	334.0	**1H$^+$ebE**	94.2
1H$^+$baZ	203.4	**1H$^+$ceZ**	304.1	**1H$^+$ebZ**	115.4
1H$^+$bcE	99.5	**1H$^+$daE**	197.6	**1H$^+$edE**	256.7
1H$^+$bcZ	90.6	**1H$^+$daZ**	172.5	**1H$^+$edZ**	279.7
1H$^+$beE	194.1	**1H$^+$dcE**	94.2		

The most stable structure is that protonated on the N2 ring nitrogen, **1H$^+$ab**, the only one found in the solid state (see below). The following one is **1H$^+$aa** (21.2 kJ mol^{-1}) protonated on N1; all the remaining cations are much more unstable; it was known that aminoazines protonated on ring nitrogen atoms.[14] To this propensity of N1 and N2 to be protonated corresponds the following MEP of Lamotrigine, see Fig. 3 where the electron density follows the order N2≈N1>>N4.

2.1.1.3. Geometry of Lamotrigine. In this section we will discuss the X-ray structures of neutral Lamotrigine as reported in the CSD.[16]

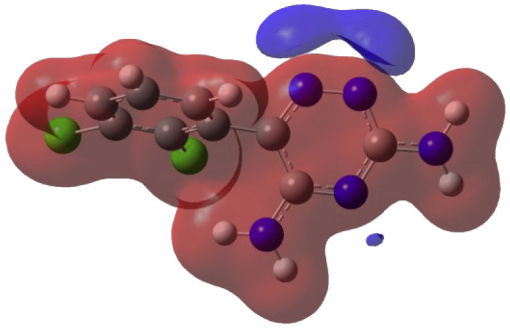

Fig. 3. The molecular electrostatic potential (MEP) of the isolated Lamotrigine. The red and blue isosurfaces correspond to +0.06 and −0.06 au, respectively.

Table S1 (Supplementary data) contains all the available information from the last update of the CSD, together with Fig. S1 reporting the formulas of some compounds of Table S1 (structures **6**–**11**).

The calculated geometry of Lamotrigine **1a** (Fig. 1) could be compared with the experimental X-ray structure (EFEMUX01) (Fig. 4).

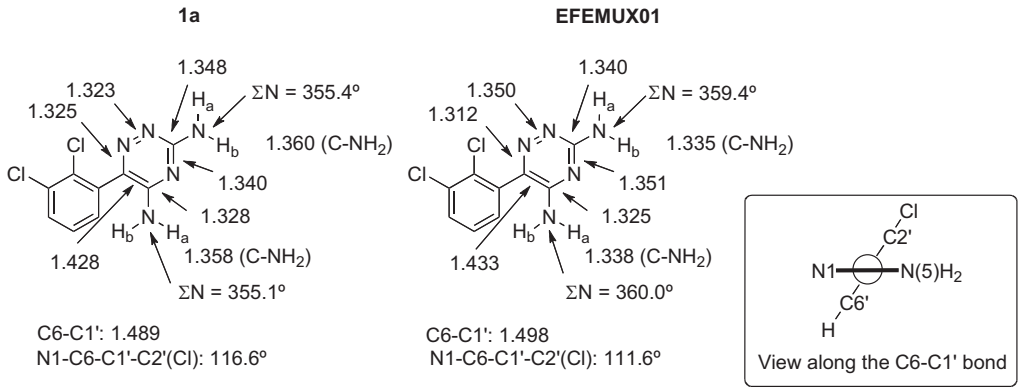

Fig. 4. Calculated and experimental geometries of Lamotrigine (distances in Å). ΣN corresponds to the sum of the three angles around the N atom (360° for an sp^2 atom and 327.8° for an sp^3 atom).

The experimental geometry is acceptably well reproduced by the calculations although the amino groups are more planar in the crystal than in the gas phase, this being probably due to the existence of intermolecular hydrogen bonds (see further on). The biaryl-type conformations[12] of **1a** and EFEMUX01 are almost identical with the chlorine atom at position 2 pointing towards the amino group at position 5.

We have calculated the barrier to the rotation about the C6–C1′ bond through a near planar structure that corresponds to a racemization process. There are two possibilities that correspond to diastereomers: that the Cl atom at position 2′ is on the side of N1 (Fig. 5a) and that it is on the side of the 5-NH_2 (Fig. 5b). The barriers are almost the same, 61.9 and 62.1 kJ mol^{-1}, respectively, therefore in the range that can be measured by dynamic NMR (DNMR) in the presence of a chiral additive or by dynamic chiral HPLC at low temperatures (cryo-chromatography).

The N1–C6–C1′–C2′(Cl) torsion angles are −14.3° for a and +174.5° for b. The amino groups are no longer sp^2 but intermediate between sp^2 and sp^3, especially in a.

Concerning the intermolecular hydrogen bonds (IMHB), excluding the frequent cases where the HB involves the 'solvent' molecule, all possibilities of homodimers are found (Fig. 6). We have named them from the amino group (positions 3 and 5) to the ring nitrogen atoms [N(2) and N(4)], for instance, 3,2/3,2 corresponds to two bonds from the amino group at position 3 to the nitrogen atom at position 2. Only a heterodimer is found in the case

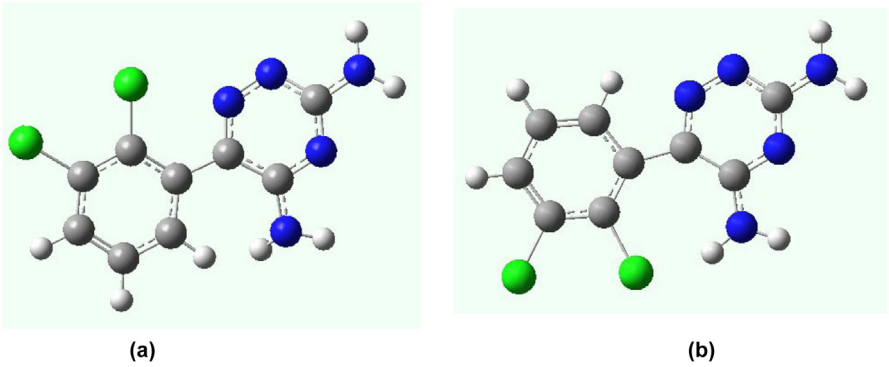

Fig. 5. The two transition states for racemization.

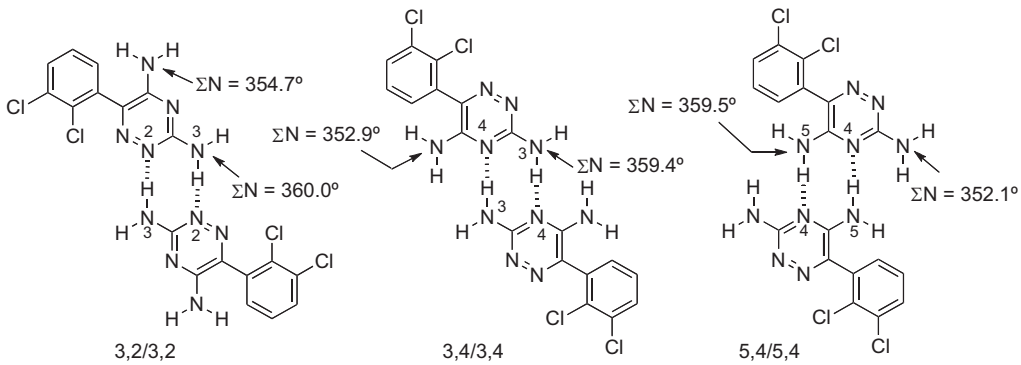

Fig. 6. Hydrogen-bonded homodimers of tautomer **1a**.

of EFEMUX01 (5,2/3,4). There is also an example of a crystal containing two homodimers, BEGZUI, thus, it will appear two times in the list given below.

The distribution of homodimers in the compounds of Table S1 is:

3,2/3,2: BEGZUI, SAXHUW; total 2.
3,4/3,4: SAXJAE, WUVKII, WUVLIJ, WUVLOR; total 4.
5,4/5,4: BEGZUI, KADPAG, OVUMEY, PEZKEM, SAXHOQ, YERTAR; total 6.

The relative energy calculations of the three homodimers (the interaction energies correspond to those of the dimer minus twice those of the monomer, always **1a**) are given below; all values in kJ mol^{-1}.

3,2/3,2=0.0 (interaction energy: −58.9)
3,4/3,4=29.4 (interaction energy: −29.5)
5,4/5,4=23.7 (interaction energy: −35.2)

As it can be seen the calculated order of stability is 3,2/3,2>>5,4/5,4>3,4/3,4 while the frequency in crystals is 5,4/5,4>3,4/3,4>3,2/3,2, but the experimental set is too small to draw any firm conclusion.

It is worth noticing that the planarity of the amino groups in the dimers is larger in those involved in HBs (about 359.6°) than in those not involved (352.7°) in agreement with Fig. 4 data, where the calculated monomer corresponds to the free NH_2 while the crystal structure (EFEMUX01) corresponds to hydrogen-bonded NH_2 groups.

Compound **9** (see Supplementary data) owing to the 2-methyl substituent has a reduced number of possible isomers (Fig. 7). Its structure (VIYQAW) corresponds to **9d*E*** (amino–imino tautomer of *E* configuration). Assuming that the relative energies should be similar to those calculated for the 2*H*-tautomers and since the most stable is the **b*E*** isomer, the relative energies are **9b*E*** (0.0), **9b*Z*** (24.9), **9d*E*** (32.3), **9d*Z*** (17.8), **9f*EE*** (25.6), **9f*EZ*** (38.3), **9f*ZE*** (28.2) and **9f*ZZ*** (36.3 kJ mol^{-1}). It appears that **9d*E*** is one of the less stable isomers. Taking into account that when replacing an N2–H by an N2–Me some stabilizing interactions may be lost, we have calculated the relative energies of the eight compounds of Fig. 7: **9b*E*** (0.0), **9b*Z*** (27.1), **9d*E*** (35.8), **9d*Z*** (21.4), **9f*EE*** (28.5), **9f*EZ*** (41.0), **9f*ZE*** (31.6), and **9f*ZZ*** (39.4 kJ mol^{-1}) that are very similar excluding the above hypothesis.

2.1.1.4. Geometry of protonated Lamotrigine. Since there are many available structures (Table S1), all of them corresponding to the **1H$^+$ab** structure, we have selected the simplest anions, chloride (YUCRAQ) and nitrate (YUCREU, two independent molecules). The comparison between calculated and experimental results (Fig. 8) is acceptable. The amino groups, both in the calculated and the crystallographic structures, are almost perfectly sp^2 and more planar than in the neutral molecules of Fig. 5. This fact and the very long C5–C6 bond suggest the major participation of the resonance structure represented on the right side of Fig. 8.

We have calculated the barrier to the rotation about the C6–C1′ bond of **1H$^+$ab**. We have obtained 66.9 kJ mol^{-1} (Cl atom at position 2′ is on the side of N1) and 69.6 kJ mol^{-1} (Cl atom on side of the 5-NH_2). Compared to the 61.9 and 62.1 kJ mol^{-1} barriers of **1a**, both show an increase; the fact that the increase of the second barrier is larger (7.5 instead of 5.5 kJ mol^{-1}) is due to an increase in the planarity of the 5-amino group (from 355.1° to 359.9°, Figs. 4 and 8, respectively).

The conformation about the C6–C1′ bond is like in the neutral molecule (chlorine towards the NH_2) for the two independent molecules of the nitrate of Lamotrigine, YUCREU

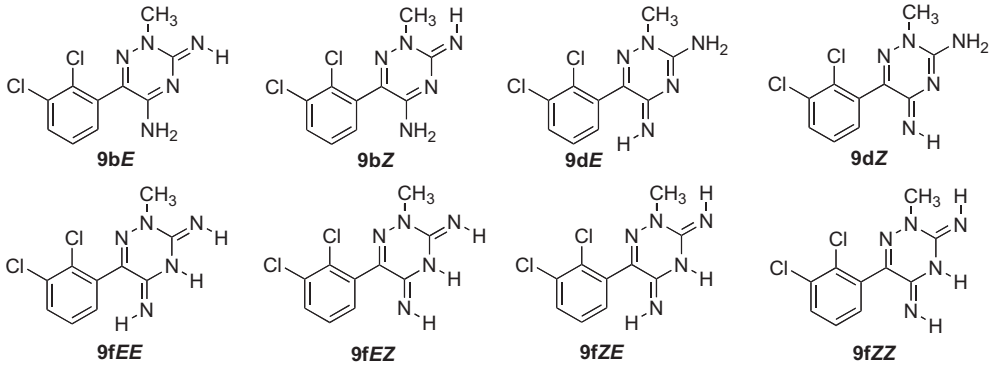

Fig. 7. The eight possible tautomers and isomers of 2-methyl Lamotrigine.

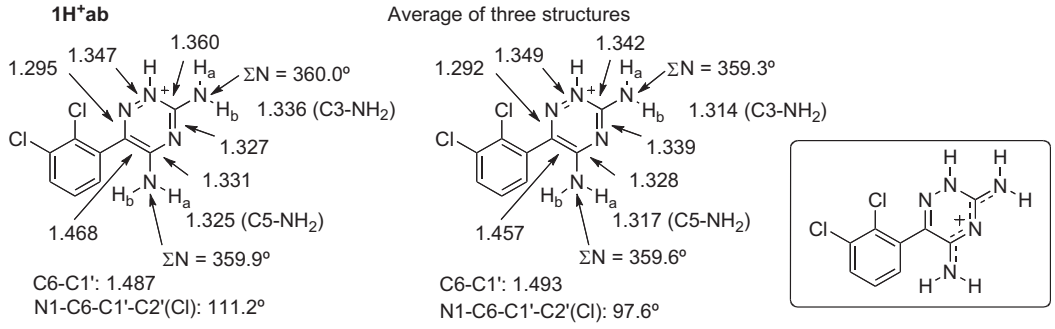

Fig. 8. The geometry of protonated Lamotrigine.

[N1–C6–C1′–C2′(Cl)=111.6°] but in the chloride, YUCRAQ, the Cl at position 2′ point towards the $N(2)H^+$ group [N1–C6–C1′–C2′(Cl)=−72.4°].

For the cations (tautomer **1H$^+$ab**), besides interaction with the 'solvents', interactions with the anions are predominant, being the one involving the $NH^+(2)$ the only one observed. In the case of cations, only the 5,4/5,4-homodimer has been found (Fig. 6).

Compounds **10** and **11** (see Table S1) have a **1H$^+$ab** type structure with the proton of the N^+–H at position 2 replaced by a methyl group (**10**) or by an *iso*-propyl group (**11**).

To compare **1a** and **1H$^+$ab** we have calculated the Wiberg indices within the NBO analysis (Fig. 9).

Note that to the very long C5–C6 bond (neutral 1.428 Å, cation 1.468 Å) correspond bond orders of 1.19 and 1.08, i.e., close to single bond. The only distances that can be compared are the C–N bonds because there are six of them, that is, 12 points for both molecules. There is a rough relationship between bond distance and bond order: bond distance=1.51–0.13 bond order, R^2=0.88.

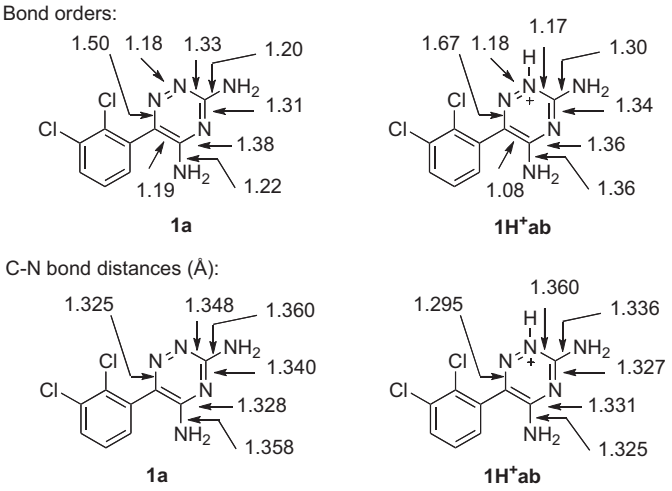

Fig. 9. NBO analysis. Double bond, bond order≈2; single bond, bond order≈1.

To get additional data about the structure of protonated Lamotrigine, the structures of two new solvated salts with saccharine as counter-anion have been determined by X-ray diffraction. While a crystal structure of a nonsolvated Lamotrigine saccharinate is already known (WUVKOO in S1),[17] the asymmetric unit of the new salts contains, together with a Lamotrigine saccharinate unit, two half 1,4-dioxane molecules (LMSC-dio) or one tetrahydrofuran (LMSC-THF).

Both crystal structures form chains of Lamotrigine dimers alternated with saccharinate dimers (Fig. 10). Molecules in the same dimer interact by stacking while two hydrogen bonds join contiguous dimers. The stacking interactions are formed by the dichlorobenzene and the benzene rings in the Lamotrigine and the saccharinate, respectively. The hydrogen bonds involve N2 and N3 as acceptors in a NH···N and a NH···O interaction, respectively, with the saccharinate, giving rise to the same $R_2^2(8)$ motif already observed in WUVKOO01. This supramolecular motif is very common in Lamotrigine salts, being systematically present in the large family of dicarboxylates.[18] Stacking of chlorobenzene rings in Lamotrigine is also observed in other crystal structures, including that of the Lamotrigine itself (EFEMUX01).[19]

In both LMSC-dio and LMSC-THF these chains are arranged in layers, appearing CH···Cl interactions between neighbor chains in the same layer. CH···O and stacking interactions between saccharinates are observed in LMSC-dio and LMSC-THF, respectively, giving rise to a different conformation of the chains inside the layer in both cases. However, the most important difference between both crystal structures is in the arrangement of the layers in the crystal packing.

In LMSC-dio, chains in neighbor layers are parallel (Fig. 11). The layers are connected by two NH···O bonds, one of them part of a $R_4^2(8)$ motif involving two Lamotrigine and two saccharinate moieties. The two symmetry independent solvent molecules are in interstices between the layers, bridging them through two NH···O bonds in one case, and through CH···π interactions with two triazine rings in the other.

In LMSC-THF, chains in neighbor layers are crisscrossed (Fig. 12). Solvent molecules are in interstices between layers, bridging them by NH···O contacts. While there is no hydrogen bonding between layers, the proximity of an oxo-group in the saccharine to the

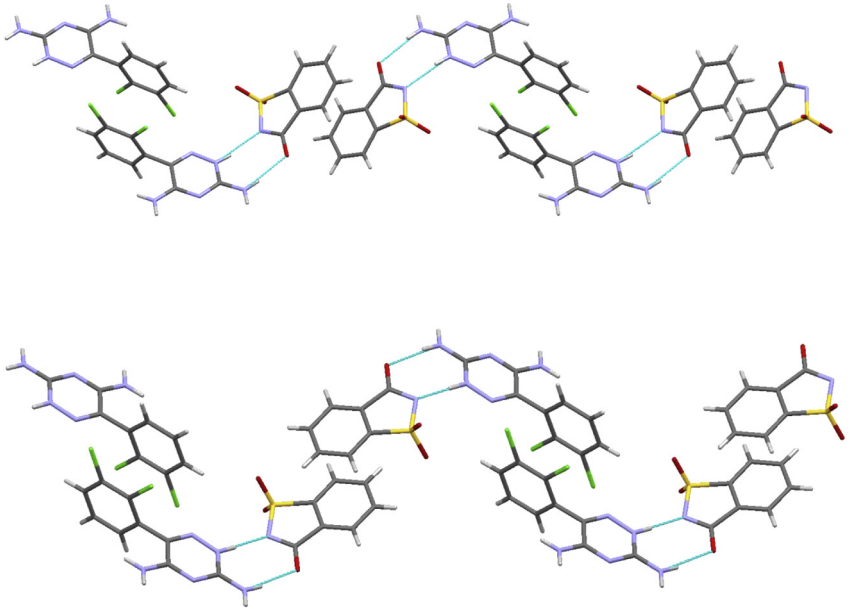

Fig. 10. Chains of Lamotrigine and saccharinate in the crystal structures of LMSC-dio (top) and LMSC-THF (bottom). Hydrogen bonds are marked with blue lines.

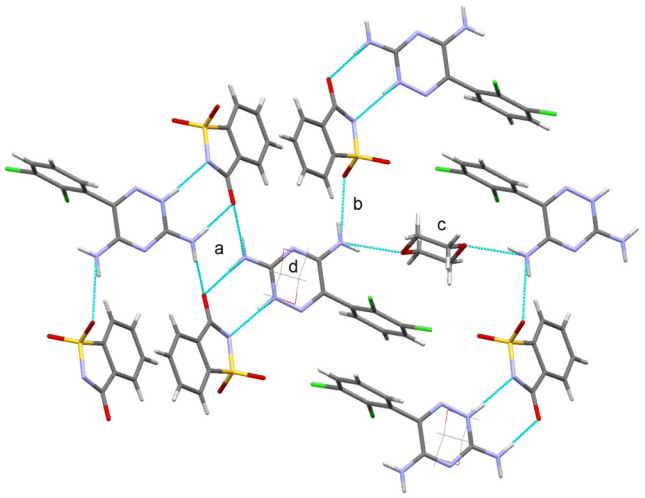

Fig. 11. Detail of the interactions between layers in LMSC-dio. Two chains fragments in different layers are plotted. The inter-layer contacts are (a) the $R_4^2(8)$ motif, (b) NH···O bond, (c) 1,4-dioxane bridging both chains. The 1,4-dioxane molecules forming CH···π bonds with one chain are sketched (d).

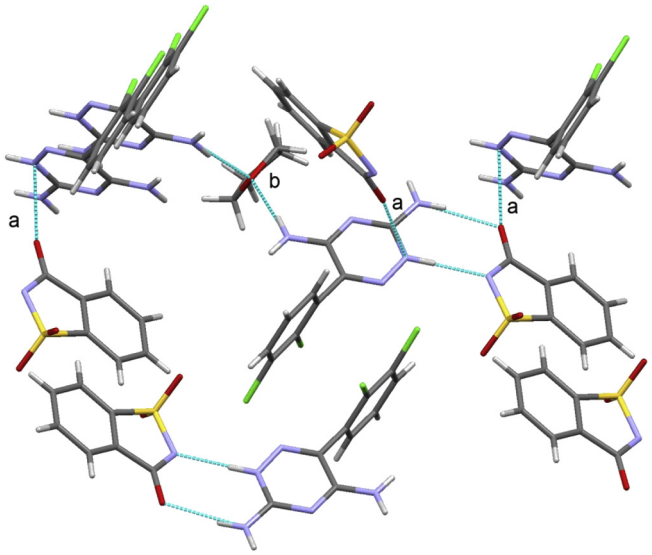

Fig. 12. Detail of the interaction between layers in LMSC-THF. One chain fragments and its contacts with one of the contiguous layers are plotted. The inter-layer contacts are (a) lone pair···π, identified by a short O···N distance and (b) THF molecule bridging two chains. Each of the molecules in the contiguous layer belongs to a different chain.

triazine ring suggests the formation of an inter-layer lone pair···π interaction.[20]

2.1.2. NMR chemical shifts

2.1.2.1. Neutral Lamotrigine. All the data are gathered in Table 3.

The ^{1}H NMR spectrum of Lamotrigine has been published four times (always in DMSO-d_6).[9,21–23] Only the signal of H5 was assigned because it is a triplet, those of H4 and H6 as well as both NH_2 groups were unassigned. The averaged values are 7.35±0.02 (H4′ or H6′), 7.43±0.02 (H5′), 7.69 (H6′ or H4′), 6.42±0.03, and 6.68±0.03 ppm (NH_2 protons). The coupling constants of the ABC system are $^3J_{HH}$=7.9±0.1 (7.69 and 7.43), $^3J_{HH}$=7.6±0.1 (7.35 and 7.43), and $^4J_{HH}$=1.65 Hz (7.43 ppm). The $^4J_{HH}$ coupling constant of 6.3 Hz reported in Ref. 9 is obviously wrong. From the spectrum they reported, a value of $^4J_{HH}$ about 2 Hz can be estimated.

The assignment of the signals of the spectrum we determined was carried out using 2D-experiments (HSQC and HMBC). The literature data were assigned by analogy.

The GIAO calculated absolute shieldings [transformed into chemical shifts by means of equation δ^1H=31.0−0.97 σ^1H (see computational details)] of the three protons of the *o*-dichlorophenyl group (7.20H5′, 7.33H6′, and 7.43 ppm H4′) are not in good agreement with the experimental results (there is even a crossing) but since the experimental data are from dichloromethane and dimethylsulfoxide solutions, we calculated the GIAO/PCM(CD_2Cl_2) and the GIAO/PCM(DMSO) absolute shieldings and transformed them into chemical shifts.

In DMSO, the calculated signals of the amino groups are at higher fields but this is expected for these protons,[24] very sensitive to concentration and solvent. What is more interesting is the difference in broadening between them. This may be due to a difference in the rotation rate about the C–N bond, the broader corresponding to the slower rate, but we carry out B3LYP/6-311++G(d,p) calculations and the barriers are almost the same, 55.0 (H towards N2) and 59.2 (H towards N4) kJ mol^{-1} for the 3-amino and 58.5 (H towards C6) and 51.1 (H towards N4) kJ mol^{-1} for the 5-amino group. Another possibility was that the anisochrony of the protons would be very different (the broader should correspond to the larger $\Delta\delta$); according to the GIAO calculations in the 3-amino group the protons are separated by 0.59 and 0.60 ppm, while in the 5-amino group, the separation is only 0.38 and 0.34 ppm. Therefore, the broad signals were assigned to the 5-amino group.

^{13}C results in DMSO-d_6 have been reported twice: in Ref. 9 the following values are given: 128.5, 130.6, 130.7 (CH of C4, C5, and C6), 131.6, 132.0, 136.8, 138.3 (C of C3, C6 of the triazine, C2, C3 of the phenyl ring), 154.1 and 162.1 ppm (C of C3, C5). In another paper only unassigned eight signals were reported with almost identical chemical shifts: 128.4, 130.6, 131.6, 132.0, 136.8, 138.3, 154.1, and 162.1 ppm (probably the 130.6 ppm signal corresponds both to the 130.6 and 130.7 of the preceding paper).[22] In the solid state (CPMAS) the resolution was less good and only signals at 129.3, 132.6, 140.2, 154.4, and 161.7 ppm were observed[22] that roughly correspond to the average of DMSO-d_6 pairs save for the carbon atoms bearing amino groups. In Table 3 are also reported our experimental assigned values. Since the X-ray structure of Lamotrigine corresponds to **1a**, the CPMAS data must correspond to **1a** and since the values in the solid state are very similar to those in DMSO-d_6 we must conclude that they also correspond to **1a**.

Often the carbon atoms bearing chlorine atoms are not well reproduced by the calculations,[25,26] so assuming a 'chlorine effect' the following equation is found that includes both ^{1}H and ^{13}C NMR data determined in CD_2Cl_2: Exp. CD_2Cl_2=(0.999±0.001) Calcd CD_2Cl_2 −(7.5±1.1) Cl, n=14, R^2=0.9999. Similar negative values for the 'chlorine effect' were found in other publications.[26,27]

In Table 3 are reported the calculated ^{15}N NMR chemical shifts. Note the considerable solvent effects on N1 and N2 and the good agreement of the three experimental chemical shifts with the calculated values for structure **1a** in DMSO.

2.1.2.2. Protonated Lamotrigine. The ^{1}H NMR spectra of protonated Lamotrigine have been reported[21] for different anions (Table 4): in average the signals appear at 7.79* (H4 or H6), 7.44 (H5), 7.68* (H6 or H4), and 6.06 ppm (a NH_2) with coupling constants of $^3J_{HH}$=7.8 (7.79), $^3J_{HH}$=7.6 (7.68), and $^4J_{HH}$=1.65 Hz. The authors named these cations ammonium salts and represented them with structure **1H$^+$ad**, but according to our calculations this structure is 120.3 kJ mol^{-1} above **1H$^+$ab** (Table 2). The calculated chemical shifts show the same problems as in the neutral molecule concerning H6 and the amino groups. But here the situation is more complex because the authors, without proof, assign to the cations

Table 3
Chemical shifts (δ, ppm) and $^1H-^1H$ coupling constants (Hz) of Lamotrigine

Atom	Calcd gas phase	Calcd CD_2Cl_2	Calcd DMSO-d_6	Exp. CD_2Cl_2	Exp. DMSO-d_6	Exp. DMSO-d_6	Exp. DMSO-d_6	Exp. CPMAS
Ref.	This work	This work	This work	This work	This work	9	22	22
H4′	7.43	7.64	7.69	7.66 J=7.6 J=2.0	7.71 J=8.0 J=1.6	7.70 J=7.8 J=6.5	7.70	—
H5′	7.20	7.45	7.48	7.44 J=7.6 J=7.6	7.45 J=8.0 J=7.6	7.45 J=7.8 J=7.8	7.42	—
H6′	7.33	7.32	7.33	7.42 J=7.6 J=2.0	7.37 J=7.6 J=1.6	7.37 J=7.6 J=6.3	7.35	—
3-NH_2	4.67, 4.07 aver. 4.37 $\Delta\delta$=0.60	4.77, 4.39 aver. 4.58 $\Delta\delta$=0.38	4.78, 4.44 aver. 4.61 $\Delta\delta$=0.34	5.15 (b)	6.45 (b)	6.46 (b)	6.69	—
5-NH_2	4.03, 3.69 aver. 3.86 $\Delta\delta$=0.34	4.64, 4.05 aver. 4.34 $\Delta\delta$=0.59	4.72, 4.12 aver. 4.42 $\Delta\delta$=0.60	4.93 (vb)	6.71 (vb)	6.72 (vb)	6.43	—
C3	159.4	161.0	161.4	161.8	162.5	162.1	162.1	161.7
C5	150.6	151.0	151.3	154.1	154.5	154.2	154.1	154.4
C6	139.0	139.8	140.3	139.3	138.7	138.3	138.3	140.2
C1′	140.0	138.4	138.1	135.4	132.4	135.8	136.8	140.2
C2′ (Cl)	139.5	140.2	140.2	132.1	132.0	131.6	131.6	132.6
C3′ (Cl)	141.6	140.9	140.8	133.8	137.2	132.0	132.0	132.6
C4′	130.1	131.6	132.0	131.4	131.6	130.7	130.6	129.3
C5′	126.9	128.5	128.8	128.3	128.9	128.5	128.4	129.3
C6′	131.6	131.5	131.6	130.1	128.9	130.6	130.6	129.3
N1	57.8	38.0	33.9	—	N.o.	—	—	—
N2	−70.6	−89.2	−92.6	—	−97.7	—	—	—
N4	−183.3	−185.6	−185.4	—	−176.5	—	—	—
3-NH_2	−316.1	−314.4	−314.2	—	−305.0[a]	—	—	—
5-NH_2	−314.6	−310.2	−308.8	—	N.o.	—	—	—

[a] $^1J_{NH}$=88.4 Hz.

Table 4
Chemical shifts (δ, ppm) and $^1H-^1H$ coupling constants (Hz) of protonated Lamotrigine. Experimental data: ^1H;[21] ^{13}C.[22] The experiments of the present work correspond to a mixture of 0.6 mL of CH_2Cl_2 and 0.4 mL of CF_3CO_2H (as internal reference $CHDCl_2$ was used)

Atom	Calcd gas phase **1H$^+$aa**	Calcd gas phase **1H$^+$ab**	Calcd gas phase **1H$^+$ad**	Calcd DMSO **1H$^+$aa**	Calcd DMSO **1H$^+$ab**	Calcd DMSO **1H$^+$ad**	Exp. CH_2Cl_2+CF_3CO_2H	Exp. DMSO-d_6	Exp. CPMAS
Ref.	This work	This work	This work	This work	This work	This work	This work	21,22	22
H4′	8.01	7.93	7.93	7.88	7.82	7.83	7.80 ^3J=8.2 ^4J=1.6	7.79[a] J=7.8	—
H5′	7.61	7.55	7.55	7.60	7.54	7.58	7.52 $^3J\approx$7.9 $^3J\approx$7.9	7.44	—
H6′	7.00	7.16	7.31	7.36	7.39	7.41	7.42 ^3J=7.7 ^4J=1.6	7.68[a] J=7.6	—
N^+H	10.49 (H1)	8.81 (H2)	6.07 (NH_3^+)	10.79 (H1)	9.23 (H2)	6.41 (NH_3^+)	[b]		—
3-NH_2	5.40	5.04	6.07 (NH_3^+)	5.42	5.40	6.41 (NH_3^+)	6.29 (b)	6.08[a](2H)	—
5-NH_2	5.21	5.60	5.30	5.38	5.59	5.34	7.24 (b)	6.08[a](2H)	—
C3	160.4	150.3	147.4	160.7	151.1	151.0	156.5	155.0	155.4
C5	155.2	153.5	152.3	155.7	153.4	153.1	154.6	158.0	155.4
C6	136.4	142.8	153.6	135.7	140.0	151.1	139.7	138.4	139.2
C1′	123.3	127.4	130.0	126.0	131.4	133.9	129.7	128.0	130.0
C2′ (Cl)	140.4	139.0	138.0	139.0	139.6	138.8	132.1	132.2	133.1
C3′ (Cl)	147.2	145.8	145.2	140.2	141.7	141.6	135.1	138.4	139.2
C4′	138.8	137.0	136.4	142.4	134.4	133.8	134.1	131.6	133.1
C5′	130.2	129.4	129.7	129.8	129.4	129.5	129.4	131.4	130.4
C6′	127.0	128.4	129.3	131.0	131.2	130.8	129.8	130.6	130.4
N1	−135.7	−37.8	46.4	−133.3	−38.6	30.2	N.o.	—	—
N2	−126.4	−225.2	−74.7	−131.1	−222.2	−79.0	N.o.	—	—
N4	−167.1	−177.8	−171.1	−172.0	−179.5	−162.2	−179.8	—	—
3-NH_2	−301.4	−311.0	−322.8	−302.7	−307.2	−325.4	−283.2[c]	—	—
5-NH_2	−296.7	−284.6	−295.4	−293.8	−285.8	−295.9	−279.8[d]	—	—

[a] Unassigned.
[b] Under the TFAA signal.
[c] $^1J_{NH}$=94.8 Hz.
[d] $^1J_{NH}$=93.8 Hz.

a structure with an amino (position 5) and an ammonium group (position 3). Assuming that the structure is **1H$^+$ab** an amino group and the N(2)$^+$H are not observed. Thus, ^{1}H NMR cannot be used to establish whether the structure of protonated Lamotrigine as **1H$^+$ab** or **1H$^+$ad** or even **1H$^+$aa**.

The ^{13}C NMR spectrum of he cyclohexylsulfamate of Lamotrigine has been reported by Khan et al.[22] (note that the anion has not aromatic carbons that could interfere). They reported the values both in DMSO-d_6 and in the solid-state but only of eight carbons instead of nine. We assumed that the signal of C3(Cl) was not observed (it was expected at about 145 ppm) because it appears together with another signal. The closest signals are those at 138.4 ppm (about 7 ppm, DMSO-d_6) and at 139.2 ppm (about 6 ppm, CPMAS). Since the authors do not assign the signals to the different carbons, those of Table 4 are only tentative, in particular for the CPMAS spectrum (a typo error reported 55.4 instead of 155.4).[22]

According to the calculations (see Supplementary data) there are only seven isomers that have two signals in the 150–160 ppm region (between parentheses, the relative energies of Table 2 in kJ mol^{-1}): **1H$^+$aa** (21.2), **1H$^+$ab** (0.0), **1H$^+$ad** (120.3), **1H$^+$dd** *E*/*Z* (~230) and **1H$^+$ea** *E*/*Z* (~100).

We have compared the nine points of the neutral (see above), the 18 points of the cation (DMSO and CPMAS) and three possible cations using the square correlation coefficient, R^2, as a criteria: **1H$^+$aa**, 0.62; **1H$^+$ab**, 0.91 and **1H$^+$ad**, 0.84. If instead of the values calculated for the gas phase we use those of PCM (DMSO) then the values are R^2, **1H$^+$aa**, 0.59; **1H$^+$ab**, 0.94 and **1H$^+$ad**, 0.80. In the case of the best correlation coefficient (**1H$^+$ab**) we have obtained Exp.=−(21±8)+(1.15±0.06) Calcd DMSO −(5.1±1.2) Cl, n=27, R^2=0.942. The equation is similar to that found for the neutral from alone (see before).

Our data (0.6 mL of CH_2Cl_2 and 0.4 mL of CF_3CO_2H) are also reported in Table 4. The signals of C3 and C5 are unambiguously assigned since both show long distance correlations with the NH_2 signal at 6.29 ppm, while C1′ and C6 show correlation peaks with the NH_2 group at 7.24 ppm. This also identifies both amino groups as reported in Table 4, respectively, 3-amino and 5-amino.

The GIAO calculated ^{15}N chemical shifts for the three structures previously discussed are reported in Table 4. Unfortunately only the less indicative signals are observed (N4, 3-NH_2, and 5-NH_2) almost useless to determine the structure of the cation. Considering that the calculations correspond to DMSO and the experimental values to CH_2Cl_2+CF_3CO_2H, the agreement is very good. In the literature we have found the following chemical shifts and coupling constants that are consistent with those we have reported in Tables 3 and 4.[28]

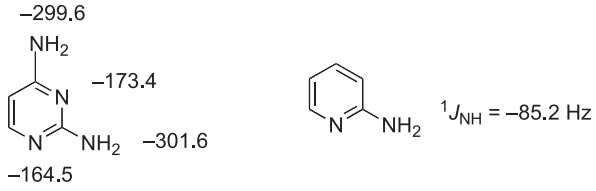

The solvent effects are not very important particularly for **1H$^+$ab** the most probable structure for the protonated Lamotrigine. On the other hand the tautomeric structures are easily differentiated.

2.1.3. Determination of the enantiomerization barrier. To determine the enantiomerization rate constant we have used DNMR. Since there are not groups giving rise to diastereotopic signals, DNMR was performed in the presence of a chiral additive in the solvent. The additive was ABTE [α,α′-bis (trifluoromethyl)-9,10-anthracendimethanol] that we have used successfully in a number of previous works.[29–31] Obviously, the use of ABTE prevent using solvents like DMSO-d_6 where Lamotrigine is soluble and solvents like $CDCl_3$ or CD_2Cl_2 become imperative. In these solvents the solubility of Lamotrigine is very poor, besides the signal of the $CHCl_3$ present in $CDCl_3$ interferes so finally CD_2Cl_2 was selected.

Using this technique (see Experimental section) we have determined a value of $\Delta G^{\ddagger}_{TC}$=62.4 kJ mol^{-1}. With less precise values, we have calculated in $CDCl_3$ a $\Delta G^{\ddagger}_{TC}$=63 kJ mol^{-1}. Compared with the calculated barriers of 61.9 and 62.1 kJ mol^{-1} for **1a**, the agreement is excellent. Similar barriers, between 58 and 68 kJ mol^{-1}, have been measured for 2-(2′-substituted-aryl)pyridines.[12]

We should note that the barrier was determined on the ABTE···Lamotrigine complex but since the hydrogen bond linking both species would take place on N2 (see previously), since these barriers are essentially of steric origin,[12] and since the populations of both complexes, being diastereomers, are not exactly 50/50 but very close to equal populations, we can safely assume that the measured barrier should be very close to that of isolated Lamotrigine.

Since Lamotrigine receptors are obviously chiral, possibly only one enantiomer will adequately fit (the eutomer) but the other (the distomer) will rapidly enantiomerize to the eutomer.

2.1.4. Aromaticity. To complete the characterization of Lamotrigine **1a** and its conjugated cation **1H$^+$ab** we have calculated their aromaticity. Two criteria have been used: the geometric using HOMA[32,33] and the NMR using NICS.[34] According to HOMA (benzene=1.00), Lamotrigine has a value of 0.92 and its cation a value of 0.66, the last one being much less aromatic. The order of aromaticity is benzene>**1a**>>**1H$^+$ab**. The bond that deviates the most from an aromatic bond[33] is the C5–C6 one (standard value 1.388 Å)[33] with values of 1.428 Å for **1a** (Fig. 4) and 1.468 Å (Fig. 8) for **1H$^+$ab**. Note that the deviation is greater for the cation in agreement with its lower aromaticity; also that the character of this bond corresponds to the resonance form depicted in Fig. 8.

The NICS values are reported in Table 5.

Table 5
Calculated NICS (ppm) values (0 Å, 1 Å, 2 Å). Face a opposite to the Cl substituents; face b on the same side than the Cl substituents

	Benzene[35]	Neutral **1a**	Cation **1H$^+$ab**
NICS (0)	−8.05	−7.36	−13.59
NICS (1) face a	−10.22	−12.25	−6.05
NICS (1) face b	−10.22	−11.69	−7.31
NICS (2) face a	−4.84	−10.68	−8.96
NICS (2) face b	−4.84	−8.75	−6.78

NICS(1) is in general a good compromise between the perturbations involved in NICS(0) and the low values of NICS(2). The order of aromaticity **1a**>benzene>>**1H$^+$ab**, being in reasonable good agreement with the HOMA conclusions.

3. Conclusions

We have completed an exhaustive survey of Lamotrigine and its monoprotonated derivatives. Although the most stable structures are those expected from previous works, particularly X-ray crystallography, we have provided information about less stable tautomers, noting that imino tautomers are protected in some patents.[36] Besides, for Lamotrigine metabolites and derivatives, our present work should be relevant.

We have reported NMR signals to identify the different structures emphasizing the usefulness of ^{15}N NMR spectroscopy. Two new solvated Lamotrigine saccharinates, one with 1,4-dixoane and the other with tetrahydrofuran, are described.

We have determined by DNMR in the presence of ABTE, the racemization barrier of Lamotrigine (62.4 kJ mol^{-1}) in perfect agreement with the calculated value. Since enantiomerization is very fast, the fact that Lamotrigine is a racemate does not seems relevant for its biological properties.

4. Experimental section

4.1. General

The anhydrous crystalline Lamotrigine used for the NMR studies and for the preparation of the salts used in the crystallographic studies was obtained as a complimentary sample from a local pharmaceutical company. The crystals were obtained like in our previous work on Lamotrigine solvates.[18]

4.2. Computational methods

The geometry of the systems under investigation has been optimized at the B3LYP[37,38]/6-311++G(d,p)[39] computational level. Frequency calculations have been carried out to ascertain the structure of the minima (IF=0) and the transition states (IF=1). The Natural Bond Orbital (NBO) method,[40,41] within the NBO-6 program,[42] has been used to calculate the bond indexes of the systems. All the calculations have been performed with the Gaussian-09 program,[43] including the molecular electrostatic potential (MEP) of neutral Lamotrigine. Absolute chemical shieldings have been calculated within the GIAO approximation[44,45] on the B3LYP/6-311++G(d,p) geometries. PCM calculations[46] were carried out as implemented in Gaussian 09. We have transformed the absolute shieldings (σ, ppm) into chemical shifts (δ, ppm) using two empirical equations we have established previously:

$$\delta^{1}H = 31.0-0.97\sigma^{1}H^{47}$$

$$\delta^{13}C = 175.7-0.963\sigma^{13}C^{48}$$

4.3. X-ray structure determination

For LMSC-THF, a 1:1 mixture of Lamotrigine (50 mg) and saccharine (36 mg) was dissolved in tetrahydrofuran by heating up to 65 °C. The solution was allowed to cool and evaporate at room temperature. Crystals suitable for single-crystal X-ray diffraction analysis were obtained after one day. Single-crystal X-ray diffraction data was collected at room temperature using a Nonius CAD4 diffractometer. Data reduction was performed with XCAD4,[49] crystal structure was solved by direct methods with SHELXS97,[50] and the DIFABS[51] absorption correction was applied.

For LMSC-dio, a 1:1 mixture of Lamotrigine (50 mg) and saccharine (36 mg) was dissolved in 1,4-dioxane by heating up to 65 °C. The solution was allowed to cool and evaporate at room temperature. Crystals suitable for single-crystal X-ray diffraction analysis were obtained after one week. Single-crystal X-ray diffraction data was collected at 300(2) K using a Nonius Kappa CCD diffractometer equipped with an Oxford Cryosystems cryostream. Data reduction and cell refinement were performed with DENZO and SCALEPACK.[52] An empirical absorption correction was applied using SORTAV.[53] Crystal structure was solved by charge flipping with SUPERFLIP.[54]

In both cases, crystal structure was refined with the SHELX-97 package.[50] H-atoms were introduced in calculated positions with the exception of the H-atom in the triazine ring, which was located in the Fourier difference maps. Non-H atoms were refined anisotropically and H-atoms were refined riding on their parent atoms. In the case of LMSC-dio, exchanging the positions of the O-atom with one of the C-atoms in the 1,4-dioxane molecule not forming hydrogen bonds does not modify significantly the crystal structure. R_1 [$I>2\sigma(I)$] increases slightly from 0.0793 to 0.0796 or 0.0799 after the positions exchange. Thus, the position of the O-atoms in this molecule could not be ascertained with certainty. The WinGX[55] package suite and Mercury[56] were used for the preparation of the publishing material. Further details on the crystal structure solution and refinement are given in Table 6.

Table 6
Selected crystallographic data for compounds LMSC-THF and LMSC-dio

	LMSC-THF	LMSC-dio
Radiation	MoKα (λ=0.71073 Å)	MoKα (λ=0.71073 Å)
Empirical formula	$C_{18}H_{16}Cl_2N_6O_5S$	$C_{20}H_{20}Cl_2N_6O_5S$
Formula weight	950.66	527.38
Crystal system	Monoclinic	Triclinic
Space group	C2/c	P-1
a/Å	26.856(5)	8.0183(4)
b/Å	7.852(2)	11.2415(6)
c/Å	21.670(4)	13.5038(9)
α/°		94.338(2)
β/°	118.63(2)	103.314(2)
γ/°		92.252(2)
Cell volume/Å^3	4010.6(14)	1179.07(12)
Z	8	2
Density calcd/Mg m^{-3}	1.574	1.485
Absorption coefficient/ mm^{-1}	0.466	0.409
F(000)	1952	544
Crystal size/mm	0.25×0.25×0.09	0.23×0.12×0.07
Theta range for data collection/°	1.73–24.98°	3.57–22.28°[a]
Index ranges	$-28\le h\le 31$, $0\le k\le 9$, $-25\le l\le 0$	$-8\le h\le 8$, $-11\le k\le 11$, $-13\le l\le 14$
Reflections collected	3638	8144
Independent reflections	3530 [R(int)=0.0533]	2953 [R(int)=0.0355]
Completeness to θ max (%)	99.9	98.5
Max. and min. transmission	0.959 and 0.892	0.972 and 9.923
Data/restraints/ parameters	3530/0/280	2953/0/307
Goodness-of-fit on F^2	1.030	1.100
R_1, wR_2 [$I>2\sigma(I)$]	0.0579, 0.1198	0.0793, 0.2388
R_1, wR_2 (all data)	0.1295, 0.1440	0.0999, 0.2545
Largest diff. peak and hole/e Å^{-3}	0.468 and −0.330	1.375 and −0.472

[a] Because of the low quality of the crystals, data could not be collected up to 25°.

4.4. Static and dynamic NMR (DNMR) experiments and experiments of enantiodifferentiation

A first analysis of ^{1}H NMR spectrum of Lamotrigine on $CDCl_3$ showed the superposition of the signals of the compound with the residual absorption of non deuterated solvent ($CHCl_3$). 0.7 mL of CD_2Cl_2 (99.90% deuteration) were added to 16 mg of Lamotrigine powder. The suspension was sonicated and heated at 30 °C during 20 min. The suspension was filtered and used to make the NMR experiments. Experiments of enantiodifferentiation were carried out after the addition of 6 mg of (*S*,*S*)-α,α′–bis(trifluoromethyl)-9,10-anthracenedimethanol (S,S-ABTE and S,S-D8-ABTE) (Figs. 13 and 14). The NMR spectrum allows us to determine a ratio [ABTE]/[Lamotrigine]=5.4 and calculating a weight of 0.13 mg of substrate in the tube of NMR. All spectra were obtained and analyzed at several temperatures between 250 and 290 K. All experiments were acquired on a Bruker AVANCE spectrometer (Bruker BioSpin, Rheinstetten, Germany) operating at 600.13 MHz proton frequency, equipped with a 5 mm inverse probe and a *z*-axis pulsed field gradient accessory. The NMR spectra (1D and 2D correlation spectra) of Lamotrigine using DMSO-d_6 and a mixture CD_2Cl_2/

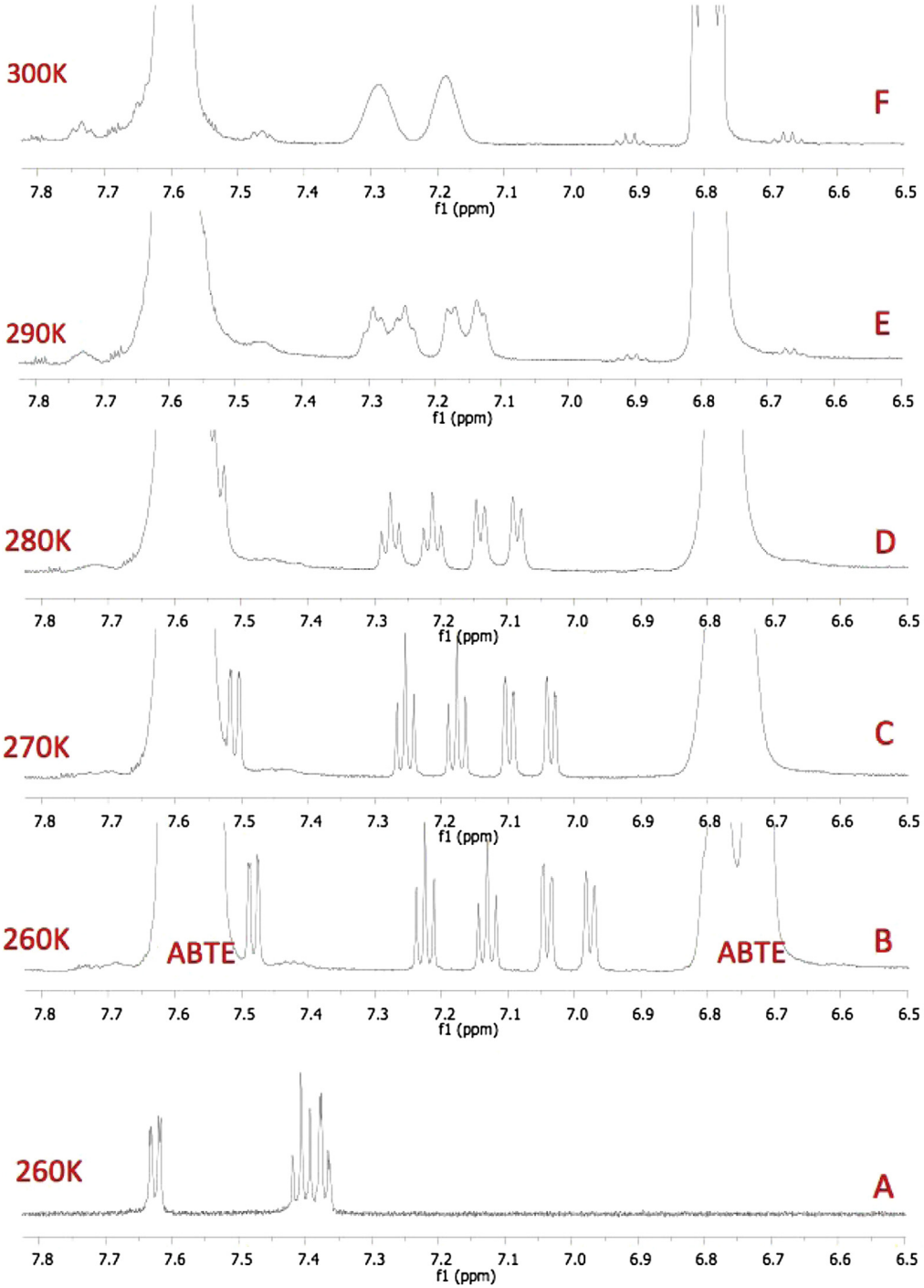

Fig. 13. 1H NMR (600 MHz, CD_2Cl_2) of Lamotrigine and effect of addition of ABTE at different temperatures (B–F). The A spectrum corresponds to a sample without ABTE.

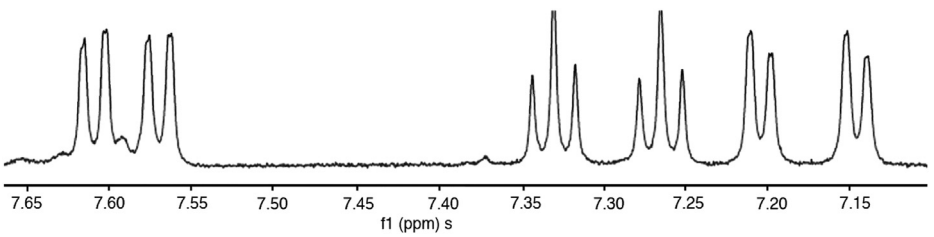

Fig. 14. [1]H NMR (600 MHz, CD_2Cl_2) of Lamotrigine and effect of addition of deuterated ABTE at 260 K using ABTE perdeuterated on the anthracene ring (ratio ABTE-d_8/Lamotrigine=3.6).

CF_3CO_2H (3:2) were obtained on a Bruker AVANCE spectrometer (Bruker BioSpin, Rheinstetten, Germany) operating at 500.13 MHz proton frequency, equipped with a 5 mm CryoProbe triple resonance and a *z*-axis pulsed field gradient accessory.[57]

Using the calculation formula for the rate constant for a coupled site (Eq. 1) and the Eyring equation (Eq. 2)[58] we have calculated the barrier for Lamotrigine plus ABTE in CD_2Cl_2,

$$k_C = \pi/2 \left[\Delta\nu^2 + 6J_{AB}^2\right]^{0.5} \quad (1)$$

$$\Delta G^{\ddagger}_{TC} = 19.12^{*}TC^{*}(10.32 + \log TC/k_C) \quad (2)$$

with $\Delta\nu$=56.175 Hz and J_{AB}=7.85 Hz measured at 260 K and a coalescence temperature TC=300 K. This lead to a value of $\Delta G^{\ddagger}_{TC}$=62.4 kJ mol^{-1}. With less precise values (the signal of $CHCl_3$ interferes) we have calculated in this solvent a $\Delta G^{\ddagger}_{TC}$=63 kJ mol^{-1}.

Acknowledgements

Thanks are also given to the Ministerio de Economía y Competitividad of Spain (Projects CTQ2012-13129-C02-02 and ENE2012-36368-C02-02), the Comunidad Autónoma de Madrid (Project MADRISOLAR2, Ref. S2009/PPQ-1533) and the Generalitat de Catalunya (Grant 2009SGR-203). Gratitude is also due to the CTI (C.S.I.C.) and CESGA for an allocation of computer time. Financial support to MICINN (project CTQ2012–32436) is gratefully acknowledged. J.G. thanks CSIC and European Social Fund for a PhD grant. We thank to the Servei de Ressonncia Magnetica Nuclear, Universitat Autónoma de Barcelona, for allocating instrument time. Dr. John E. Davies is acknowledged for single crystal X-ray diffraction data collection.

Supplementary data

Supplementary data related to this article (^{1}H, ^{13}C, and ^{15}N NMR. Spectra of Lamotrigine in CD_2Cl_2 at different temperatures). Optimized Cartesian coordinates, corresponding energies and absolute shieldings for species discussed in the text. CCDC-969425 (for LMSC-dio), and CCDC-969426 (for LMSC-THF) contain the supplementary crystallographic data for this paper. These data can be obtained free of charge from The Cambridge Crystallographic Data Centre via www.ccdc.cam.ac.uk/data_request/cif. Supplementary data related to this article can be found at http://dx.doi.org/10.1016/j.tet.2014.02.075.

References and notes

1. Engel, J.; Pedley, T. A. In *Epilepsy. A Comprehensive Textbook Lippincott Williams & Wilkins, Wolters Kluwer: Philadelphia, 2008*.
2. Wyllie, E.; Cascino, G. D.; Gidal, B. A.; Goodkin, H. P. In *Wyllie's Treatment of Epilepsy: Principles and Practice Lippincott Williams & Wilkins, Wolters Kluwer: Philadelphia, 2011*.
3. International League Against Epilepsy (ILAE), www.ilae.org.
4. Gil-Nagel, A.; López-Muñoz, F.; Serratosa, J. M.; Moncada, I.; García-García, P.; Álamo, C. *Seizure* **2006**, *15*, 142–149.
5. Goodwin, F. K. *J. Clin. Psychiatry* **2003**, *64*, 161–174.
6. Hirschfeld, R. M. A. *Guideline Watch: Practice Guideline for the Treatment of Patients with Bipolar Disorder*, 2nd ed.; American Psychiatric Association: Arlington, VA, 2005.
7. Calabrese, J. R.; Huffman, R. F.; White, R. L.; Edwards, S.; Thompson, T. R.; Ascher, J. A.; Monaghan, E. T.; Leadbetter, R. A. *Bipolar Disord.* **2008**, *10*, 323–333.
8. Goodwin, F. K.; Jamison, K. R.; Ghaemi, S. N. *Manic-depressive Illness: Bipolar Disorders and Recurrent Depression*, 2nd ed.; Oxford University: New York, 2007.
9. Beattie, K.; Phadke, G.; Novakovic, J. *Lamotrigine, Profiles of Drug Substances, Excipients, and Related Methology*, 2012, Vol. 37, pp 245–284.
10. Seridi, L.; Boufelfel, A. *J. Mol. Liq.* **2011**, *158*, 151–158.
11. Ramya, T.; Gunasekaran, S.; Ramkumaar, G. R. *Spectrochim. Acta, Part A* **2013**, *114*, 277–283.
12. Alkorta, I.; Elguero, J.; Roussel, C.; Vanthuyne, N.; Piras, P. *Adv. Heterocycl. Chem.* **2012**, *105*, 1–188.
13. Guidelines on the Use of INNs for Pharmaceutical Substances, 1997.
14. Elguero, J.; Marzin, C.; Katritzky, A. R.; Linda, P. *The Tautomerism of Heterocycles*; Academic: New York, NY, 1976; p 165.
15. Stanovnik, B.; Tisler, M.; Katritzky, A. R.; Denisko, O. V. *Adv. Heterocycl. Chem.* **2006**, *91*, 1–134.
16. CSD Database Version 5.35 (Nov. 2013) Allen, F. H. *Acta Crystallogr., Sect. B* **2002**, *58*, 380–388 Allen, F. H.; Motherwell, W. D. S. *Acta Crystallogr., Sect. B* **2002**, *58*, 407–422.
17. Cheney, M. L.; Shan, N.; Healey, E. R.; Hanna, M.; Wojtas, L.; Zaworotko, M. J.; Sava, V.; Song, S.; Sanchez-Ramos, J. R. *Cryst. Growth Des.* **2010**, *10*, 394–405.
18. Galcera, J.; Friščić, T.; Hejczyk, K. E.; Fábián, L.; Clarke, S. M.; Day, G. M.; Molins, E.; Jones, W. *CrystEngComm* **2012**, *14*, 7898–7906.
19. Sridhar, B.; Ravikumar, K. *Acta Crystallogr., Sect. C* **2009**, *65*, o460–o464.
20. Egli, M.; Sarkhel, S. *Acc. Chem. Res.* **2007**, *40*, 197–205.
21. Qian, Y.; Lv, P.-C.; Shi, L.; Fang, R.-Q.; Song, Z.-C.; Zhu, H.-L. *J. Chem. Sci.* **2009**, *121*, 463–470.
22. Rahman, Z.; Zidan, A. S.; Samy, R.; Sayeed, V. A.; Khan, M. A. *AAPS PharmSciTech* **2012**, *13*, 793–801.
23. Venkanna, G.; Nagender, D.; Venkateswarlu, P.; Shekhar, K. C.; Madhusudhan, G.; Mukkanti, K. *Der Pharm. Chem.* **2012**, *4*, 100–105.
24. Pinto, J.; Silva, V. L. M.; Silva, A. M. S.; Claramunt, R. M.; Sanz, D.; Torralba, M. C.; Torres, M. R.; Reviriego, F.; Alkorta, I.; Elguero, J. *Magn. Reson. Chem.* **2013**, *51*, 203–221.
25. Claramunt, R. M.; Santa María, M. D.; Sanz, D.; Alkorta, I.; Elguero, J. *Magn. Reson. Chem.* **2006**, *44*, 566–570.
26. Alkorta, I.; Alvarado, M.; Elguero, J.; García-Granda, S.; Goya, P.; Jimeno, M. L.; Menéndez-Taboada, L. *Eur. J. Med. Chem.* **2009**, *44*, 1864–1869.
27. Santa María, M. D.; Claramunt, R. M.; Herranz, F.; Alkorta, I.; Elguero, J. *J. Mol. Struct.* **2009**, *920*, 323–326.
28. Berger, S.; Braun, S.; Kalinowski, H.-O. *NMR Spectroscopy of the Non-metallic Elements*; John Wiley & Sons: Chichester, UK, 1997; see Chapter 4.
29. Pomares, M.; Sánchez-Ferrando, F.; Virgili, A.; Alvarez-Larena, A.; Piniella, J. F. *J. Org. Chem.* **2002**, *67*, 753–758.
30. Comelles, J.; Estivill, C.; Moreno-Mañas, M.; Virgili, A.; Vallribera, A. *Tetrahedron* **2004**, *60*, 11541–11546.
31. Estivill, C.; Pomares, M.; Kotev, M.; Ivanov, P.; Virgili, A. *Tetrahedron: Asymmetry* **2005**, *16*, 2993–2997.
32. Kruszewski, J.; Krygowski, T. M. *Tetrahedron Lett.* **1972**, *13*, 3839–3842.
33. Krygowski, T. M. *J. Chem. Inf. Comput. Sci.* **1993**, *33*, 70–78.
34. Schleyer, P. V. R.; Maerker, C.; Dransfield, A.; Jiao, H.; van Eikema Hommes, N. J. R. *J. Am. Chem. Soc.* **1996**, *118*, 6317–6318.
35. Claramunt, R. M.; Alkorta, I.; Elguero, J. *Comput. Theor. Chem.* **2013**, *1019*, 108–115.
36. Congreve, M. S.; Andrews, S. P.; Mason, J. S.; Richardson, C. M.; Brown, G. A. US Patent 2013/0029963.
37. Becke, A. D. *J. Chem. Phys.* **1993**, *98*, 5648–5652.
38. Lee, C. T.; Yang, W. T.; Parr, R. G. *Phys. Rev. B* **1988**, *37*, 785–789.
39. Frisch, M. J.; Pople, J. A.; Binkley, J. S. *J. Chem. Phys.* **1984**, *80*, 3265–3269.
40. Reed, A. E.; Curtiss, L. A.; Weinhold, F. *Chem. Rev.* **1988**, *88*, 899–926.
41. Foster, J. P.; Weinhold, F. *J. Am. Chem. Soc.* **1980**, *102*, 7211–7218.
42. Glendening, E. D.; Badenhoop, J. K.; Reed, A. E.; Carpenter, J. E.; Bohmann, J. A.; Morales, C. M.; Landis, C. R.; Weinhold, F. *NBO 6.0*; University of Wisconsin: Madison, WI, 2013.
43. Frisch, M. J.; Trucks, G. W.; Schlegel, H. B.; Scuseria, G. E.; Robb, M. A.; Cheeseman, J. R.; Scalmani, G.; Barone, V.; Mennucci, B.; Petersson, G. A.; Nakatsuji, H.; Caricato, M.; Li, X.; Hratchian, H. P.; Izmaylov, A. F.; Bloino, J.; Zheng, G.; Sonnenberg, J. L.; Hada, M.; Ehara, M.; Toyota, K.; Fukuda, R.; Hasegawa, J.; Ishida, M.; Nakajima, T.; Honda, Y.; Kitao, O.; Nakai, H.; Vreven, T.; Montgomery, J. A., Jr.; Peralta, J. E.; Ogliaro, F.; Bearpark, M.; Heyd, J. J.; Brothers, E.; Kudin, K. N.; Staroverov, V. N.; Kobayashi, R.; Normand, J.; Raghavachari, K.; Rendell, A.; Burant, J. C.; Iyengar, S. S.; Tomasi, J.; Cossi, M.; Rega, N.; Millam, N. J.; Klene, M.; Knox, J. E.; Cross, J. B.; Bakken, V.; Adamo, C.; Jaramillo, J.; Gomperts, R.; Stratmann, R. E.; Yazyev, O.; Austin, A. J.; Cammi, R.; Pomelli, C.; Ochterski, J. W.; Martin, R. L.; Morokuma, K.; Zakrzewski, V. G.; Voth, G. A.; Salvador, P.; Dannenberg, J. J.; Dapprich, S.; Daniels, A. D.; Farkas, Ö.; Foresman, J. B.; Ortiz, J. V.; Cioslowski, J.; Fox, D. J. *Gaussian 09, Revision A.1*; Gaussian: Wallingford CT, 2009.
44. Ditchfield, R. *Mol. Phys.* **1974**, *27*, 789–807.
45. London, F. *J. Phys. Radium* **1937**, *8*, 397–409.
46. Tomasi, J.; Mennucci, B.; Cammi, R. *Chem. Rev.* **2005**, *105*, 2999–3093.
47. Silva, A. M. S.; Sousa, R. M. S.; Jimeno, M. L.; Blanco, F.; Alkorta, I.; Elguero, J. *Magn. Reson. Chem.* **2008**, *46*, 859–864.
48. Blanco, F.; Alkorta, I.; Elguero, J. *Magn. Reson. Chem.* **2007**, *45*, 797–800.
49. Harms, K.; Wocadlo, S. *CAD4 Data Reduction*; University of Marburg: Marburg, Germany, 1995.
50. Sheldrick, G. M. *Acta Crystallogr., Sect. A* **2008**, *64*, 112–122.
51. Walker, N.; Stuart, D. *Acta Crystallogr., Sect. A* **1983**, *39*, 158–166.
52. Otwinowski, Z.; Minor, W. *Macromol. Crystallogr., Part A* **1997**, *276*, 307–326.
53. Blessing, R. H. *Acta Crystallogr., Sect. A* **1995**, *51*, 33–38.
54. Palatinus, L.; Chapuis, G. *J. Appl. Crystallogr.* **2007**, *40*, 786–790.
55. Farrugia, L. J. *J. Appl. Crystallogr.* **1999**, *32*, 837–838.
56. Macrae, C. F.; Bruno, I. J.; Chisholm, J. A.; Edgington, P. R.; McCabe, P.; Pidcock, E.; Rodriguez-Monge, L.; Taylor, R.; van de Streek, J.; Wood, P. A. *J. Appl. Crystallogr.* **2008**, *41*, 466–470.
57. http://www.bruker-biospin.com/cryofit.html.
58. Sandstràm, J. *Dynamic NMR Spectroscopy*; Academic: London, UK, 1982.